Molecular Crystals and Liquid Crystals Science and Technology. Section A. Molecular Crystals and Liquid Crystals

Publication details, including instructions for authors and subscription information:
http://www.tandfonline.com/loi/gmcl19

Dynamics of Backbone Chain and Side Groups in a Nematic Liquid Single Crystal Elastomer Studied by Combined Mechanical and Stress-Optical Measurements

F. Schmidt [a], J. Siepmann [a], W. Stille [a] & G. R. Strobl [a]

[a] Fakultät für Physik, Universität Freiburg, Hermann-Herder-Str. 3, D-79104, Freiburg, Germany

Version of record first published: 24 Sep 2006

To cite this article: F. Schmidt, J. Siepmann, W. Stille & G. R. Strobl (2000): Dynamics of Backbone Chain and Side Groups in a Nematic Liquid Single Crystal Elastomer Studied by Combined Mechanical and Stress-Optical Measurements, Molecular Crystals and Liquid Crystals Science and Technology. Section A. Molecular Crystals and Liquid Crystals, 350:1, 103-123

To link to this article: http://dx.doi.org/10.1080/10587250008025237

Mol. Cryst. Liq. Cryst., Vol. 350, pp. 103-123
Reprints available directly from the publisher
Photocopying permitted by license only

Dynamics of Backbone Chain and Side Groups in a Nematic Liquid Single Crystal Elastomer Studied by Combined Mechanical and Stress-Optical Measurements

F. SCHMIDT, J. SIEPMANN, W. STILLE* and G.R. STROBL

Fakultät für Physik, Universität Freiburg, Hermann-Herder-Str. 3, D-79104 Freiburg, Germany

(Received July 27, 1999; In final form December 17, 1999)

Dynamic mechanical and stress-optical measurements on nematic liquid single elastomers have been carried out both in the nematic and in the isotropic phase. In case of shear stress and in case of tensile stress applied parallel to the director the compliances were not affected by the nematic-isotropic transition. For tensile stress oriented perpendicular an increased compliance was observed in the vicinity of the phase transition. The stress-optical coefficients for tensile stresses applied pararallel and perpendicular to the director both increase on approaching the nematic-isotropic transition. In the isotropic phase its temperature dependence is well described by the Landau-de Gennes theory. Far from the transition temperature in the nematic phase other mechanisms superpose this behavior, leading to negative stress-optical coeffients for stress parallel, and positive coefficients perpendicular to the director.

Keywords: Nematic; elastomer; dynamic mechanical properties; stress-optical coefficient; critical phenomena

INTRODUCTION

Since several years liquid crystalline elastomers[1] are the object of structural and dynamical investigations. They combine the feature of orientational order of low molar mass liquid crystals with the tendency of polymer networks to form gaussian coils. The network makes it possible to affect the liquid crystalline

* To whom correspondence should be addressed.

order by a mechanical field. The macroscopic optical features depend on order and orientation of the liquid crystalline side groups.

The combination of measurements of elastic moduli with that of the stress-optical coefficient allows to study the static and dynamical behaviour of the entire system.[2] Only on the basis of transparent samples measurements of the stress-optical coefficient are possible. Usually this condition is only given in the isotropic phase of liquid crystalline side group elastomers. In the liquid crystalline phases polydomains are formed. The polydomain samples are quite opaque due to the highly non-uniform director. Küpfer[3] prepared a liquid crystalline side group elastomer with a permanent, macroscopically uniform alignment by applying mechnical stress before the second of two crosslinking steps. These elastomers, called Liquid Single Crystal Elastomers (LSCE), are optically similar to organic or inorganic single crystals. Their optical axis is oriented parallel to the direction of mechanical stress during preparation. Here we report on structural investigations with X-ray scattering, dynamic mechanical and dynamic stress-optical measurements. The last method was also used to show the critical behaviour at the nematic-isotropic phase transition as described by the Landau-de Gennes theory.

EXPERIMENTAL

1. Samples

The samples under study were synthesised and characterised by J. Küpfer, Institut für Makromolekulare Chemie, Freiburg, using a two-step crosslinking reaction scheme.[3] Figure 1 shows their chemical structure. The mesogenic groups are attached to the polysiloxane backbone by methylene spacer groups. The number m of the spacer groups and the crosslinking density were varied as shown in Table I. The values of the crosslinking density were calculated from the amounts of the crosslinking agents. As indicated by stress-strain measurements, the density of mechanically active crosslinking points must be much lower. The phase transition temperatures were determined by DSC. The dynamic investigations are restricted to the sample LSCE4-(10 %).

2. X-ray Scattering

X-ray scattering patterns were registered on films using a Kiessig camera and Cu-K_α radiation. A special sample holder was used which allowed to study

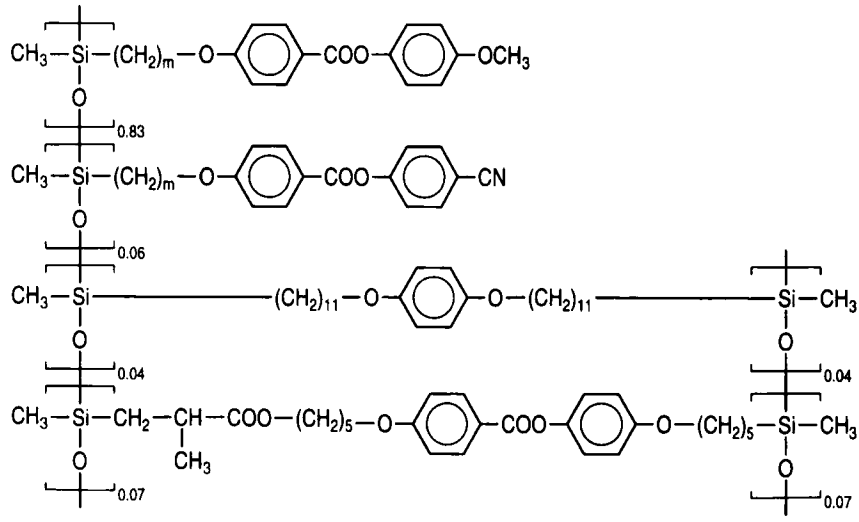

FIGURE 1 Chemical structure of LSCE*m*-(10 %)

stretched samples at temperatures up to 150 °C. The sample was placed between two clamps which were movable on a slider. Temperature control was accomplished by electrical heating and cooling with water.

TABLE I Crosslinking densities, spacer lengths, and transition temperatures of the samples (g: glassy, pc: partial crystalline)

sample	*crosslinking density [%]*	*spacer length m*	*transition temperatures [°C]*
LSCE4-(10 %)	10	4	g 4 n 86 i
LSCE6-(10 %)	10	6	g −8 n 85 i
LSCE6-(5 %)	5	6	g −7 pc 46 n 86 i

3. Optical and Mechanical Measurements

Dynamic optical and mechanical measurements probe the temperature and frequency dependence of the mechanical and optical properties of a sample. In the experiment the sample was oriented with its optical axis either parallel or perpendicular to the tensile axis. It was exposed to a stress

$$\sigma(t) = \sigma_0 + \sigma_1 e^{i\omega t}, \tag{1}$$

which consisted of a static component σ_0 applied to keep the sample stretched and a superposed sinusoidal modulated dynamic component $\sigma_1$with frequency $f = \omega/2\pi$. σ, σ_0 and σ_1 are engineering stresses, i.e., the applied forces per cross section area of the unstrained sample. The stress causes a strain

$$\varepsilon(t) = \varepsilon_0 + \varepsilon_1 e^{i(\omega t - \delta)} \tag{2}$$

and a birefringence

$$\Delta n(t) = \Delta n_0 + \Delta n_1 e^{i(\omega t - \varphi)} \tag{3}$$

in the sample, where ε_0, ε_1, Δn_0 and Δn_1 are the zeroth and the first Fourier components of the strain and the birefringence respectively, and δ and φ are phase angles. The dynamic mechanical properties of the sample will be described by the complex elastic modulus

$$E^* = E' + iE'' := \frac{\sigma(t) - \sigma_0}{\varepsilon(t) - \varepsilon_0} = \frac{\sigma_1}{\varepsilon_1} e^{i\delta}, \tag{4}$$

the dynamic stress-optical behaviour will be characterised by the dynamic stress-optical coefficient[4]

$$C^* = C' - iC'' := \frac{\Delta n(t) - \Delta n_0}{(\sigma(t) - \sigma_0)(1 + \varepsilon_0)} = \frac{\Delta n_1}{\sigma_1(1 + \varepsilon_0)} e^{-i\varphi}. \tag{5}$$

As in the case of ordinary rubbers, the stress-optical coefficient is calculated with the component of the true stress σ_1 $(1 + \varepsilon_0)$, which is given by the applied force per cross section area in the strained state (the small contribution of ε_1 is neglected).[5]

The experimental apparatus consists of a commercial mechanical spectrometer (Polymer Laboratories DMTA MK II) working in tensile geometry, with the additional implementation of an optical setup for a simultaneous determination of the birefringence. Eleven frequencies of the spectrometer in the range 0.1 Hz $\leq f \leq$ 50 Hz were used. The optical setup corresponds to that of an PCSA ellipsometer,[6] where PCSA denotes the sequence of optical elements. The beam of a He-Ne laser passes a prism polarizer (P) oriented at an angle α, a quarter-wave plate (compensator C) oriented at 45°, the sample (S), and a second polarizer (analyzer A) oriented at 45° (all angles with regard to the axis of tensile stress).

The transmitted intensity of light I, detected by a photodiode, is given as a function of the birefringence Δn and the thickness d of the sample by

$$I(\alpha, \Delta n) = \frac{I_{max}}{2} \left[1 + \sin\left(2\alpha + \frac{2\pi d}{\lambda} \Delta n\right)\right], \tag{6}$$

where I_{max} is the maximum of the transmitted intensity and λ is the wavelength of the laser light (633 nm). The birefringence Δn is given by Equation (3). In order to get a sinusoidal modulated intensity in the case of a small amplitude

sinusoidal modulated birefringence, the polarizer angle α is chosen so that $2\alpha + 2\pi d\Delta n_0/\lambda$ is a multiple of 2π. Around this operating point the sine function in Equation (6) is approximately linear. First order Taylor expansion of Equation (6) around the operating point leads to

$$I(\Delta n) \approx \frac{I_{max}}{2}\left[1 + \frac{2\pi d}{\lambda}(\Delta n - \Delta n_0)\right]. \tag{7}$$

Combination of Equation (7) and Equation (3) results in:

$$I(t) \approx \frac{I_{max}}{2}\left[1 + \frac{2\pi d}{\lambda}\Delta n_1 e^{i(\omega t - \varphi)}\right]. \tag{8}$$

Hence, for a small sinusoidal modulation of Δn when the operating point is set by adjusting α, the amplitude Δn_1 and the phase angle φ of the dynamical component of the birefringence can be determined by a measurement of the amplitude and the phase angle of the transmitted intensity. In the experiment the operating point was stabilised by controlling the angle α between the polariser and the tensile axis. $I_{\max}$ and the operation point value of α were determined by α-dependent measurements of I at the smallest strain amplitude setting, where Δn_1 can be neglected.

The intensity of the transmitted light and strain of the sample were sampled simultaneously at 64 equidistant points per period. Fast Fourier transformation on the controlling microcomputer yields the amplitudes ε_1 and Δn_1 of strain and birefringence and their relative phase angle $\psi = (\varphi - \delta)$. Using the elastic modulus measured by the mechanical spectrometer, C^* can be calculated using the Equations (4) and (5). In case of large amplitudes Δn_1 the approximation given by Equation (8) is no longer valid. Then a non-linear Levenberg-Marquardt fit[7] to the Equations (6) and (3) was used instead of the fast Fourier transform algorithm.

Static birefringence data were obtained using a Leitz Ortholux Pol II-BK polarizing microscope equipped with an adjustable tilting compensator, an additional quartz plate retarder and a heating stage.

RESULTS

1. X-ray investigations

The X-ray scattering patterns obtained for LSCE6-(5 %) in the partially crystalline, the nematic and the isotropic phase are shown in Figure 2. They are similar to those obtained for a non-crosslinked liquid crystalline polysiloxane with spac-

ers of five methylene groups[8]. In that case the structure in the partially crystalline state was found to be monoclinic with the side groups densely packed within layers and the backbone chain located between these layers. The mesogenic groups belonging to the same chain alternate regularly between two adjacent layers. In case of the elastomer, the reflexes in the partially crystalline phase are less pronounced (Figure 2a), not allowing a detailed determination of the structure. As a remarkable feature a quite sharp equatorially oriented reflex corresponding to a period of 0.3 nm shows up, which might be associated with the distance of two silicon atoms along the main chain. This would support the picture of main chains oriented perpendicular to the mesogenic groups in the crystalline parts of the sample.

In the nematic phase (Figure 2b) still diffuse layer like reflections are visible. This is typical for liquid crystalline side group polymers[8, 9] and even more pronounced in case of cyclic liquid crystalline side group oligomers[10]. Even in the isotropic phase (Figure 2c), where the orientational order nearly vanishes, some diffuse reflections at small angles are visible. There still seems to exist some tendency to form associates. The temperature dependent X-ray patterns were analysed using a procedure described by Leadbetter and Norris,[11] which allows a quantitative determination of the order parameter S. The orientational distribution function $f_d(\theta)$ of the mesogenic groups and the azimutal intensity distribution $I(\alpha)$ of the liquid-like wide angle scattering are related by

$$I(\alpha) = C \int_0^{\frac{\pi}{2}} f_d(\theta) \frac{1}{\cos^2 \alpha} (\tan^2 \theta - \tan^2 \alpha)^{-\frac{1}{2}} \sin \theta d\theta. \tag{9}$$

If the orientational distribution function is assumed to be of the Maier-Saupe form

$$f_d(\theta) = A e^{a \cos^2 \theta}, \tag{10}$$

$f_d(\beta)$ can be obtained by fitting of the parameter a. The order parameter S then follows from

$$S = \langle P_2(\cos \theta) \rangle = \frac{\int_0^1 P_2(\cos \theta) e^{a \cos^2 \theta} d \cos \theta}{\int_0^1 e^{a \cos^2 \theta} d \cos \theta} \tag{11}$$

with

$$P_2(\cos \theta) = \frac{3}{2} \cos^2 \theta - \frac{1}{2}. \tag{12}$$

Figure 3 shows order parameters obtained in this way. The values are reasonable, the experimental errors, however, are quite large.

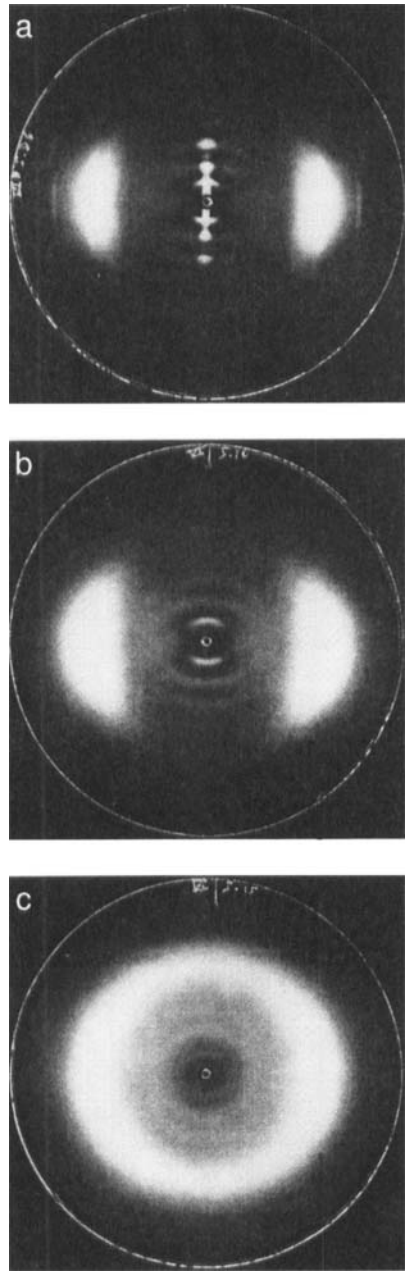

FIGURE 2 X-ray scattering patterns of LSCE6-(5 %) in the partially crystalline state at 22.5 °C (a), in the nematic phase at 66.1 °C (b) and in the isotropic phase at 104.5 °C (c). The optical axis is oriented vertically

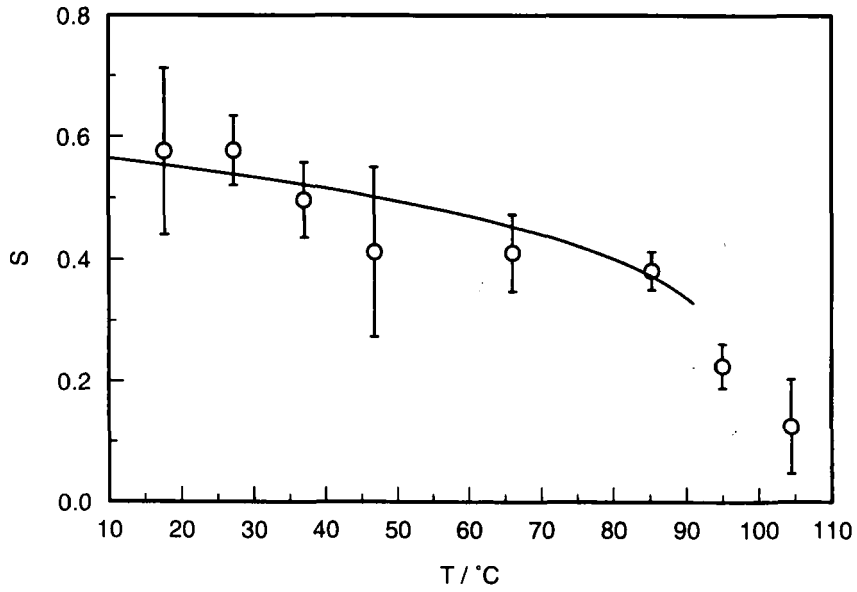

FIGURE 3 Temperature dependence of the order parameter S of LSCE6-(5 %), derived from the azimutal wide angle X-ray intensity distribution

X-ray patterns of samples stretched parallel to the director show only a slight broadening in the wide angle area and a slight increase of the period corresponding to the small angle reflexes.

When the samples are stretched perpendicular to the initial director, at a threshold strain reorientation takes place (see Figure 4). Then both the small angle and wide angle reflexes split in their azimutal orientation, corresponding to two sets of domains tilted in opposite direction against the initial orientation. At high strain values the pattern again looks like the initial one, but rotated by 90°. This behavior and the stripe domains which can be observed simultaneously are described and analyzed in detail by other authors.[12] It is consistent with the assumption of a prolate main chain conformation in equilibrium with the nematic director, which has to follow the new chain orientation at high strain values.

3. Static Birefringence

Figure 5 shows the temperature dependence of the static birefringence of Δn of LSCE6-(5 %). In the nematic phase it reflects the typical temperature depend-

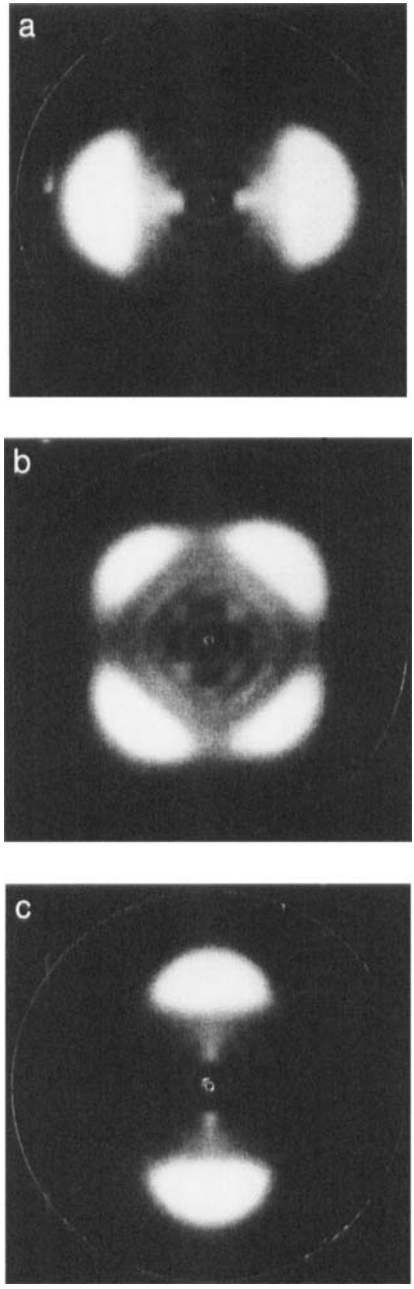

FIGURE 4 X-ray scattering patterns of LSCE4-(10 %) in the nematic phase at 21 °C, stretched by 0 % (a), 30% (b), and 75% (c)

ence of the order parameter S. The continous line in Figure 3 was obtained assuming proportionality between birefringence and order parameter. As there exist no sharp transition temperature, the obtained values do not show a discontinuous jump at the nematic-isotropic phase transition. At about 97 °C the temperature dependence changes significantly. As shown by Figure 6 and the insertion in Figure 5, above this temperature the dependence is well described by a power law

$$\Delta n = b(T - T^*)^{-1} \tag{13}$$

with $b = 0.00630$ K and $T^* = 94.80$ °C, suggesting a near-critical divergence of the static birefringence under the influence of the forces excerted by the network which retains a finite anisotropy.

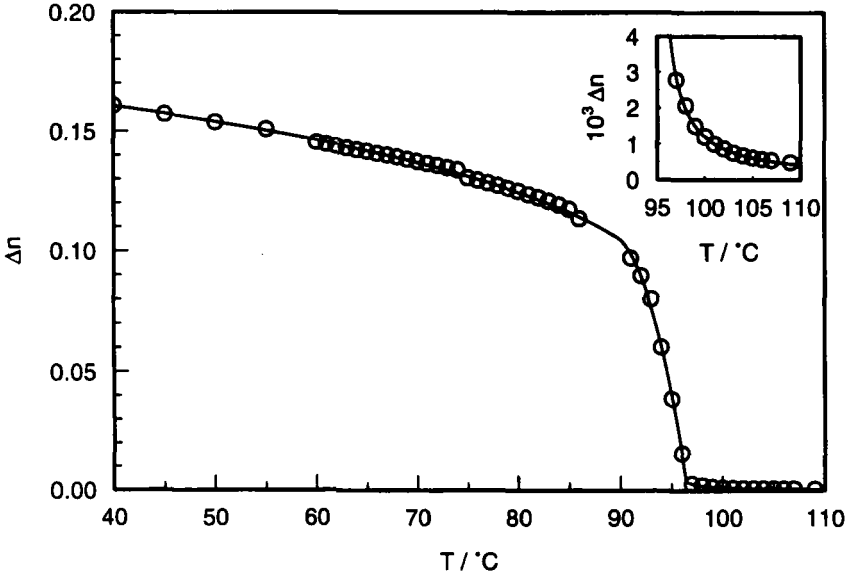

FIGURE 5 Temperature dependence of the static birefringence Δn of LSCE6-(5 %)

4. Mechanical properties

Frequency dependent measurements of the shear compliance were carried out for LSCE4-(10 %) at various temperatures in the range from −5 °C to 100 °C. Employing time-temperature superposition and applying a special algorithm[13] master curves were obtained. They are shown in Figure 7. One observes one

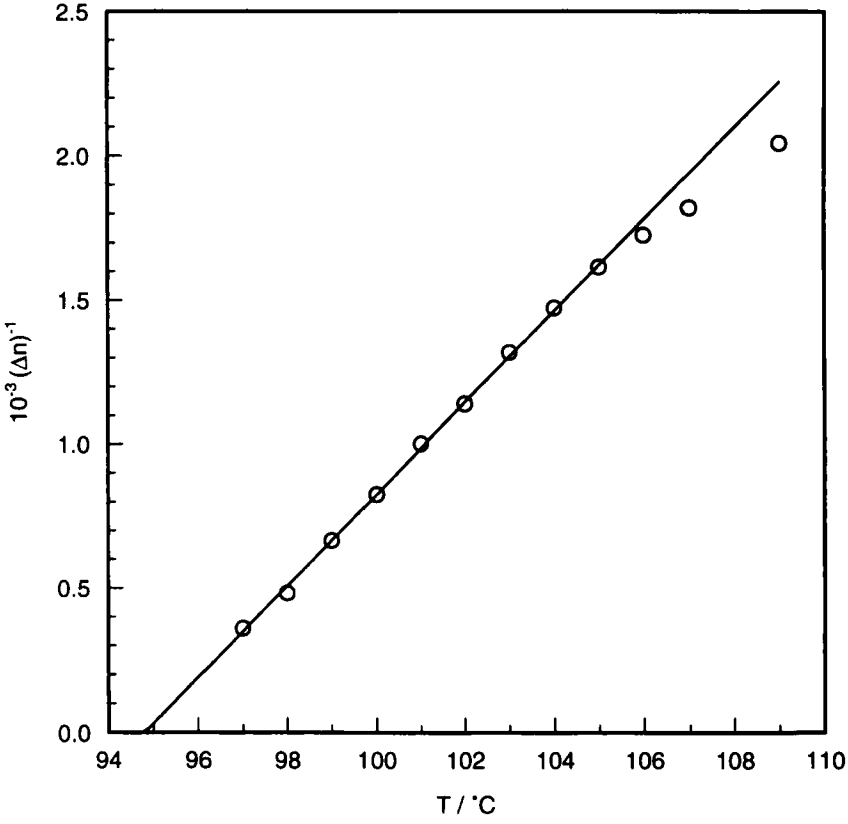

FIGURE 6 Temperature dependence of the inverse static birefringence $(\Delta n)^{-1}$ of LSCE6-(5 %) in the isotropic phase

relaxation process spanning a compliance range from 10^{-4} Pa^{-1} to 10^{-7} Pa^{-1}. The compliance expected for a glass, in the order of $10^{-9}Pa^{-1}$, is not yet reached at the lowest temperatures, which is indicative for the existence of an additional process. Such a process is known from polymethacrylates with sidegroups and there addressed as β-process.[14]

Analogous measurements were conducted under tensile stress. Figure 8 presents the tensile compliance for stresses applied parallel and perpendicular to the director, using three different frequencies. D' increases with temperature within the nematic phase and then reaches a plateau. The compliance parallel to the director (Figure 8a) is not affected by the nematic-isotropic transition, the compliance in perpendicular direction shows a peak (Figure 8b).

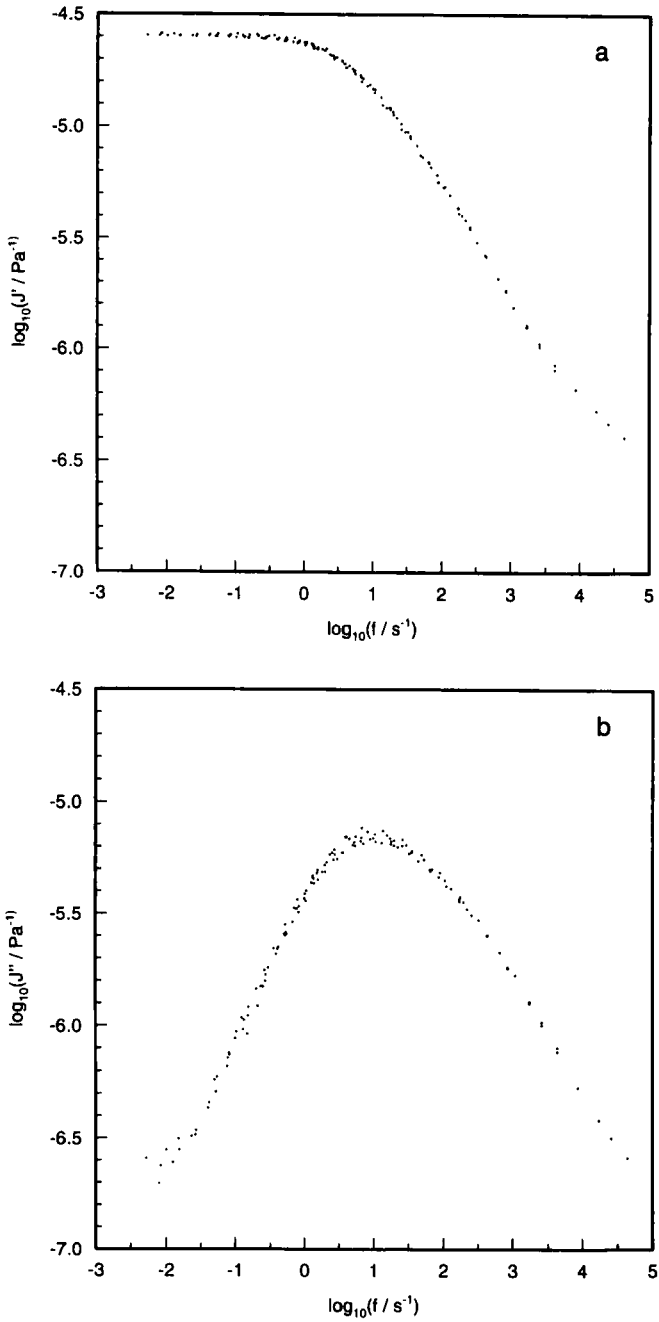

FIGURE 7 Master curve of the shear compliance of LSCE4-(10 %). (a) Real part, b) imaginary part

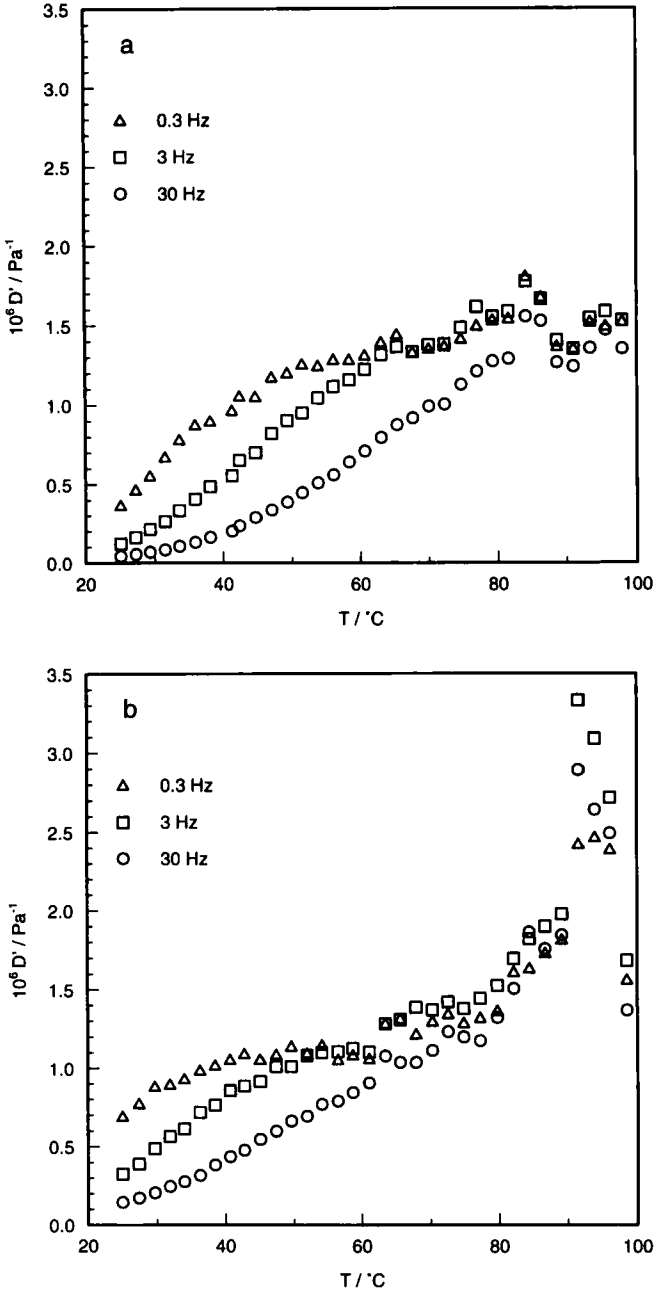

FIGURE 8 Temperature dependence of the real part D' of the tensile compliance of LSCE4-(10 %) for three different frequencies. (a) Stress parallel, (b) perpendicular to the director

5. Dynamical stress-optical coefficient

Figure 9 shows the real part C' of the stress-optical coefficient. It increases on approaching the nematic- isotropic transition temperature on both sides. In the nematic phase far from the phase transition C' is negative for tensile stresses applied parallel to the director (Figure 9a), which means, that the birefringence decreases with increasing strain in the nematic phase. This is consistent with the observation of the slight broadening of the X-ray intensity distribution with increasing strain. On the other hand, for a tensile stress applied perpendicular to the director positive values of C' are obtained (Figure 9b). The stress-optical coefficient vanishes on approaching the glass temperature.

DISCUSSION

1. Landau-de Gennes Theory

The results can be discussed within the scope of the Landau-de Gennes theory.[15]-[19] De Gennes described the free energy density f of a nematic liquid crystalline elastomer in the neighbourhood of the nematic-isotropic phase transition as a power series in the order parameter S extended by additional terms[17]

$$f = f_0 + \frac{A}{2}S^2 - \frac{B}{3}S^3 + \frac{C}{4}S^4 - USe + \frac{1}{2}Ee^2 - \sigma e, \tag{14}$$

where σ is the applied stress, ε the strain of the sample, E the static elastic modulus and U a coupling constant between strain and order parameter. The coefficients B and C are only weakly temperature dependent and therefore assumed as constant. The characteristic feature is the temperature dependence of A, given by

$$A(T) = a(T - T_C^*), \tag{15}$$

with a denoting a temperature independent constant. The temperature T_C^* is located slightly below the nematic-isotropic phase transition temperature T_C and can be determined by investigating the near-critical behaviour of the liquid crystal in the isotropic phase: the mesogens behave in the isotropic phase as if there would be a second order phase transition at T_C^*.

Minimisation of f in Equation 14 with respect to ε leads to

$$\varepsilon_{eq} = \frac{1}{E}\sigma + \frac{U}{E}S. \tag{16}$$

In addition to the applied stress, the liquid crystalline order can also affect the strain of the sample. Even if there is no external stress, a spontaneous deforma-

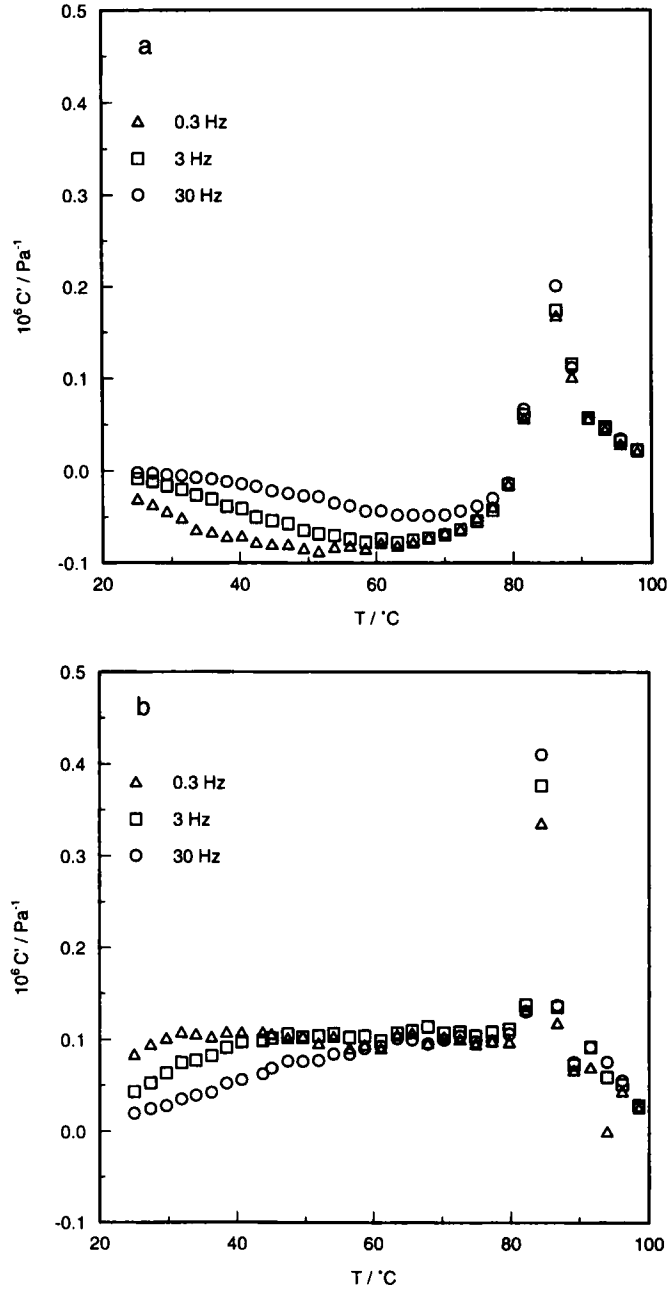

FIGURE 9 Temperature dependence of the real part C' of the stress-optical coefficient of LSCE4-(10 %) for three different frequencies. (a) Stress parallel, (b) perpendicular to the director

tion of the network occurs in the nematic phase.[20] Inserting Equation 16 into Equation 14 results in

$$f = f_0 - \frac{U}{E}\sigma S + \frac{a}{2}(T - T_N^*)S^2 - \frac{B}{3}S^3 + \frac{C}{4}S^4 - \frac{\sigma^2}{2E}, \tag{17}$$

where T_N^* is given by

$$T_N^* = T_C^* + \frac{U^2}{Ea}. \tag{18}$$

T_N^* now plays the role of T_C^* as a hypothetical second order phase transition temperature. In the isotropic phase, where S is small, the third and forth order terms in S in Equation 17 can be neglected. Minimising f with respect to S then results in the temperature dependence of the equilibrium value of the order parameter in the isotropic phase:

$$S_{eq}(T) = \frac{U\sigma}{Ea(T - T_N^*)}. \tag{19}$$

To describe the dynamical behaviour of the order parameter, de Gennes introduced the phenomenological equation[18, 21]

$$\frac{\partial S}{\partial t} = -L\frac{\partial f}{\partial S}, \tag{20}$$

where L is a phenomenological kinetic coefficient. Inserting the second order approximation of Equation 17, Equation 20 is solved by

$$S(t) = S_{eq} + (S(t_0) - S_{eq})\exp[-La(T - T_N^*)(t - t_0)]. \tag{21}$$

The stress-optical coefficient C^* exhibits the same dynamical behavior. In the frequency domain it shows up as a Debye process with the relaxation frequency

$$f_0(T) = \frac{1}{2\pi}La(T - T_N^*). \tag{22}$$

and a relaxation strength ΔC following from the proportionality

$$\Delta n \approx \Delta n_{max} S : \tag{23}$$

$$\Delta C(T) = \frac{\Delta n}{\sigma} = \frac{U\Delta n_{max}}{Ea(T - T_N^*)}. \tag{24}$$

Here Δn_{max} is the birefringence for a perfectly ordered nematic phase ($S = 1$). Equation (22) indicates a critical slowing down upon approaching T_N^*. It is accompanied by the critical divergence of the relaxation strength ΔC, expressed by Equation (24).

2. Comparison between Theory and Experiment

The frequency dependencies of the tensile compliance and the stress-optical coefficient can be fitted to Cole-Cole processes.[22] Figure 10 shows the temperature dependencies of the resulting relaxation frequencies (Figures 10a, 10b) and of the relaxation strength of the stress-optical coefficient (Figure 10c), both for stresses oriented parallel and perpendicular to the director. The relaxation strength of the stress-optical process increases on approaching the nematic-isotropic phase transition temperature from both sides. If the stress is applied perpendicular to the director both the compliance and the stress-optical coefficient are affected by the phase transition (see Figure 8b). We consider this case and therefore plot the quantity $(E\Delta C)^{-1}$ as a function of the temperature, as given in Figure 11. Applying Equation (24) in the isotropic phase, a linear temperature dependence with a slope of $a/(U\Delta n_{max})$ is expected, which is in good agreement with the experimental data. This is consistent with the temperature dependence of the static birefringence in the isotropic phase without external stress (see Figures 5, 6 and Equation 13). In that case the birefringence can be understood as the response to the internal stress produced by the two-step crosslinking procedure. This also leads to a power law temperature dependence, $\Delta n \sim (T - T_N^*)^{-1}$.

From birefringence and order parameter measurements a value of $\Delta n_{max} = 0.40$ is obtained for LSCE4-(10 %). The Landau-de Gennes parameter a can be calculated from the heat of the nematic-isotropic transition ΔH_C and the order parameter S_{C+} in the nematic phase at the transition temperature:

$$a = \frac{2\Delta H_C}{S_{C+}T_C}.$$

With $\Delta H_C = 1.38 \cdot 10^6\ \mathrm{Jm^{-3}}$ from DSC measurements and $S_{C+} = 0.32$ a value of $a = 75 \cdot 10^3\ \mathrm{Jm^{-3}\ K^{-1}}$ is obtained. With these values two slightly different coupling constants $U_{\parallel} = 33.1 \cdot 10^3\ \mathrm{Jm^{-3}}$ and $U_{\perp} = 47.7 \cdot 10^3\ \mathrm{Jm^{-3}}$ result from the slopes of the Figures 11a and 11b. The linear fits also results in two different critical temperatures, $T_N^* = 87.5\,^{\circ}\mathrm{C}$ for parallel orientation and $T_N^* = 84.0\,^{\circ}\mathrm{C}$ for perpendicular orientation of the stress.

The difference $T_N^* - T_C^*$ follows from Equation 18 by introducing U, a, and E. One obtains a small quantity, in the order of 10^{-2} K.

The temperature difference $T_C - T_C^*$ is not known exactly but can roughly estimated from the minima in the experimental values of $(E\Delta C)^{-1}$ (T) as $T_C - T_C^* \approx 1$ K, in agreement with typical values observed for low molar mass

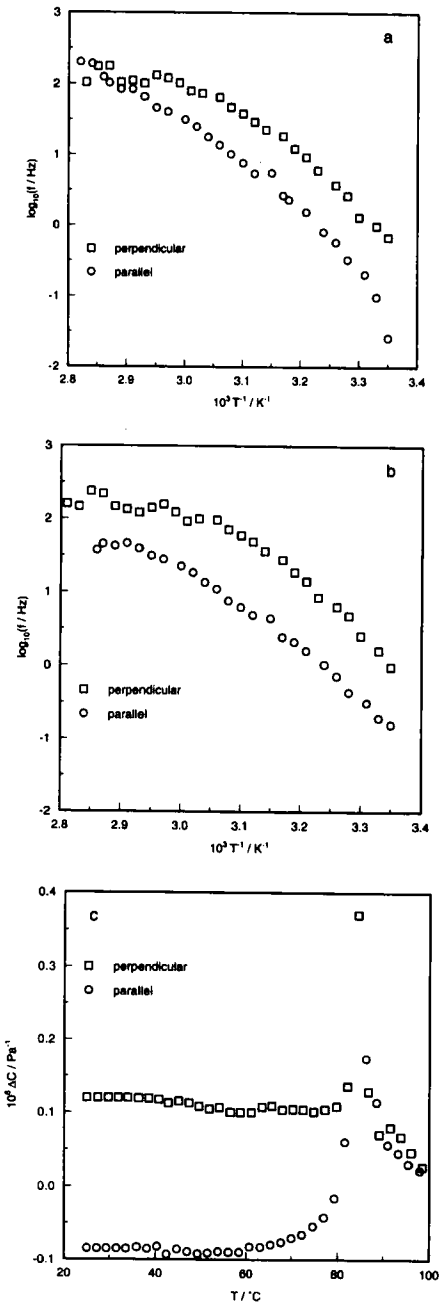

FIGURE 10 Temperature dependencies of the relaxation frequencies of LSCE4-(10 %). (a) Mechanical, (b) optical process. (c) Temperature dependence of the relaxation strength of the optical process

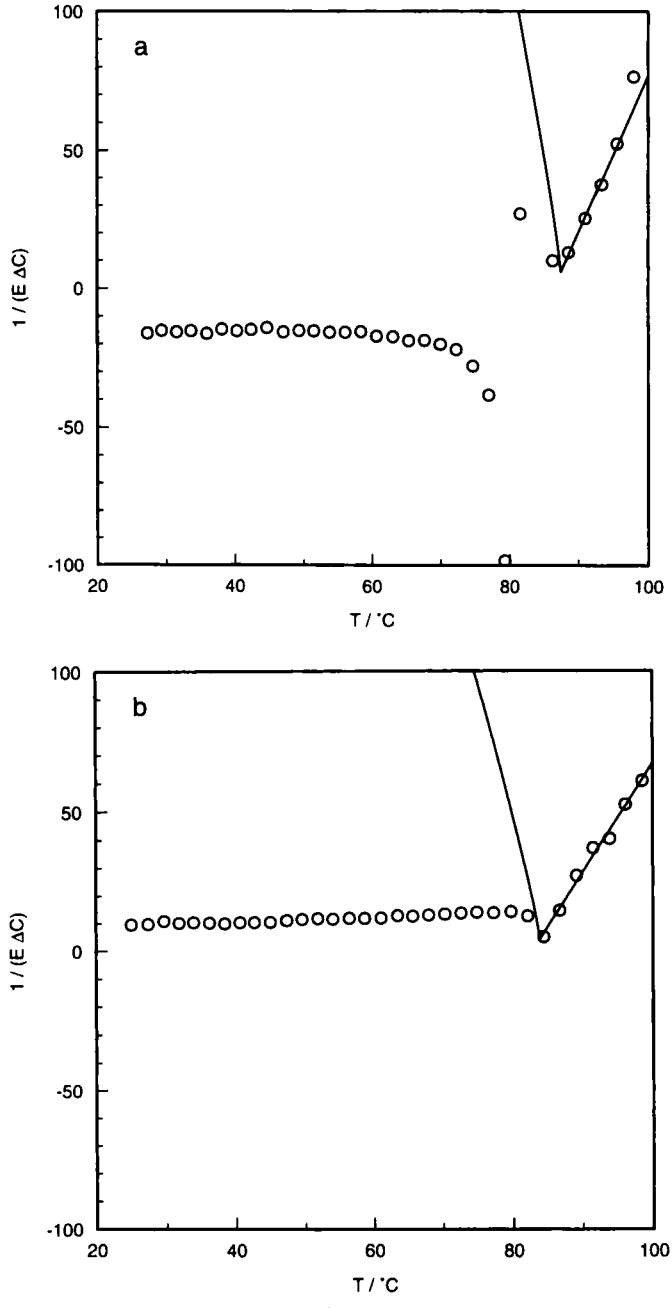

FIGURE 11 Temperature dependence of $(E\Delta C)^{-1}$ for LSCE4-(10 %). (a) Stress parallel, (b) perpendicular to the director. Solid lines: Fits to the Landau-de Gennes theory

liquid crystals. The Landau-de Gennes coefficients B and C then can be calculated using

$$B = \frac{3a(T_C - T_C^*)}{S_{C+}}$$

and

$$C = \frac{2B}{3S_{C+}} = \frac{2a(T_C - T_C^*)}{S_{C+}^2},$$

giving $B \approx 0.7 \cdot 10^6\ \mathrm{Jm^{-3}}$ and $C \approx 1.5 \cdot 10^6\ \mathrm{Jm^{-3}}$. Using these values the quantity $(E\Delta C)^{-1}$ was calculated also in the nematic phase. For this purpose Equation 17 was minimised with respect to S, resulting in a cubic equation to be solved for the equilibrium order parameter S_{eq} in the nematic phase. The stress-optical coefficient then was obtained by calculating numerically the difference quotient $\Delta S_{eq}/\Delta\sigma$ and using Equation 23. As shown in Figure 11, minima occur at the phase transition in agreement with the experiment, but the theoretical curves in the nematic phase give values much higher than the experimental data. Two reasons may be responsible. First, the Landau-de Gennes theory originates from an expansion around $S = 0$, a condition not met in the nematic phase, where a free energy expansion up to the fourth power of S seems not to be sufficient.[19] Second, as demonstrated by the negative values of the stress-optical coefficient in Figure 9a, another mechanism obviously superposes the normal reaction process. This and the slight broadening of the wide angle X-ray intensity distribution for stress applied parallel to the director may be understood as a peculiar reaction of the local director on perturbations arising in an inhomogenously crosslinked network. On the other hand, for stresses oriented perpendicular to the director, inhomogenities may lead to local reorientations of the director even below the threshold stress, resulting in a positive stress-optical response.

Acknowledgements

Support of this work by the Deutsche Forschungsgemeinschaft (Sonderforschungsbereich 428, Freiburg) is gratefully acknowledged.

References

[1] H. Finkelmann, H. J. Koch and G. Rehage, *Makromol. Chem., Rap. Commun.*, **2**, 317 (1981).
[2] R. Sigel, W. Stille, G. Strobl and R. Lehnert, *Macromolecules*, **26**, 4226 (1993).
[3] J. Küpfer and H. Finkelmann, *Makromol. Chem., Rapid. Commun.*, **12**, 717 (1991).
[4] H. Janeschitz-Kriegl, *Polymer Melt Rheology and Flow Birefringence*, (Springer, Berlin and Heidelberg, 1983).
[5] L. R. G. Treloar, *The Physics of Rubber Elasticity*, (Clarendon Press, Oxford, 1975), 3rd ed.
[6] R. M. A. Azzam and N. M. Bashara, *Ellipsometry and Polarized Light*, (North-Holland, Amsterdam, 1987).

[7] W. H. Press, S. A. Teukolsky, W. T. Vetterling and B. P. Flannery, *Numerical Recipes in FORTRAN*, (Cambridge University Press, Cambridge, 1992), 2nd ed.
[8] W. Hotz and G. Strobl, *Colloid Polym. Sci.*, **267**, 889 (1989).
[9] T. J. Bunning, H. Korner, V. V. Tsukruk, C. M. McHugh, C. K. Ober and W. W. Adams, *Macromolecules*, **29**, 8717 (1996).
[10] V. V. Tsukruk, T. J. Bunning, H. Korner, C. K. Ober and W. W. Adams, *Macromolecules*, **29**, 8706 (1996).
[11] A. J. Leadbetter and E. K. Norris, *Molecular Physics*, **38**, 669 (1979).
[12] H. Finkelmann, I. Kundler, E. M. Terentjev and M. Warner, *J. Phys. II France* **7**, 1059 (1997).
[13] J. Honerkamp and J. Weese, *Rheol. Acta* **32**, 57 (1993).
[14] N. G. McCrum, B. E. Read and G. Williams, *Anelastic and Dielectric Effects in Polymeric Solids*, (Wiley & Sons, London, 1967).
[15] L. Landau, *Phys. Z. Sowjet.*, **11**, 26 (1937).
[16] P.-G. de Gennes, *Mol. Cryst. Liq. Cryst.*, **12**, 193 (1971).
[17] P.-G. de Gennes, *C. R. Seances Acad. Sci. Paris*, **281B**, 101 (1975).
[18] P.-G. de Gennes in *Polymer Liquid Crystals*, edited by A. Ciferri, W. R. Krigbaum and R.B. Meyer, (Academic Press, New York, 1982), p. 115.
[19] P.-G. de Gennes and J. Prost, *The Physics of Liquid Crystals*, (Clarendon Press, Oxford, 1993).
[20] M. Warner in *Side Chain Liquid Crystal Polymers*, edited by C. B. McArdle, (Blackie and Son, Glasgow, 1989).
[21] M. Doi and S.F. Edwards, *The Theory of Polymer Dynamics*, (Clarendon Press, Oxford, 1986).
[22] K. S. Cole and R. H. Cole, *J. Chem. Phys.*, **9**, 341 (1941).